Fatigue Cracking and Fractography

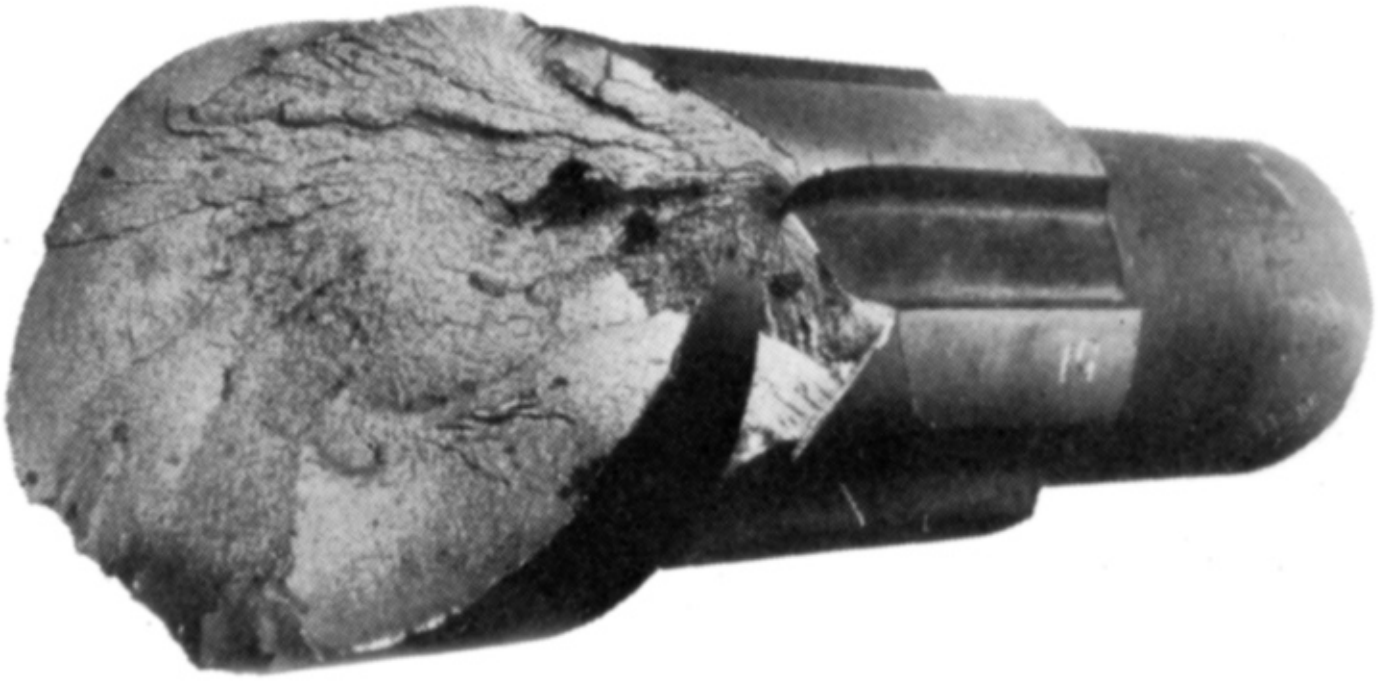

(Above) This macroscopic view of a fractured shaft shows a series of radiating ridges on the fracture surface, which can be traced along the direction in which they converge to identify the area of the fracture origin. In that area, note the darker region, which represents the initial fatigue and slow crack growth prior to final failure in one or a few load cycles. Surface crack initiation was at the bottom of a spline on the shaft, the same kind of initiation at or within a stress concentrator which is often observed.

(Far left, below) Fatigue initiation occured at the bar surface and occupied only the small, shiny area before overload failure of most of the cross-section.

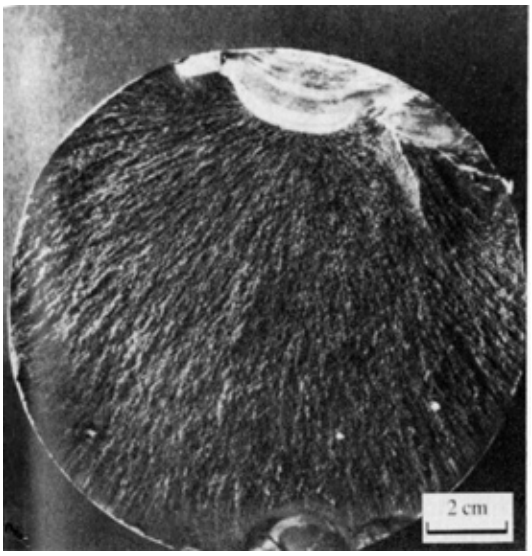

(Near left) Almost the opposite: crack initiation at the arrowed point on the bar surface, followed by crack growth across nearly all the section before overload in the small crescent at lower right. Careful examination is necessary in such examination of fractures.

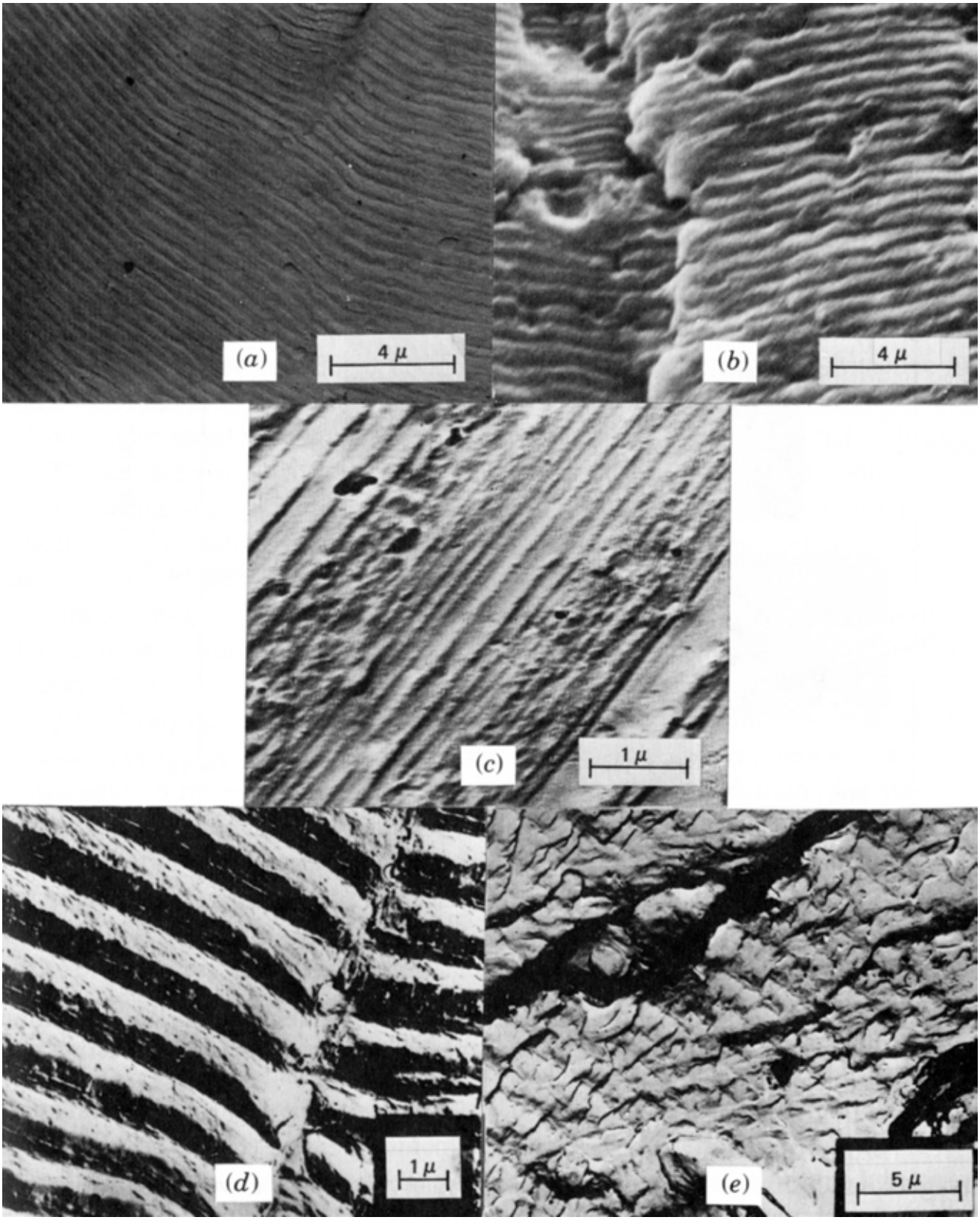

(a) Typical replica appearance of regualr striations. (b) Striations viewed in SEM. (c) Random loading produced irregular striations, varying with load amplitude, still one striation per cycle. (d) So-called "ductile" striations, with large, regular size and spacing. (e) Brittle striations, where successive crack front locations are still marked but not by the same process as in figures (a) through (d).

From Hertzberg, *Deformation and Fracture Mechanics of Engineering Materials* (4th ed.), Wiley, 1996, page 607

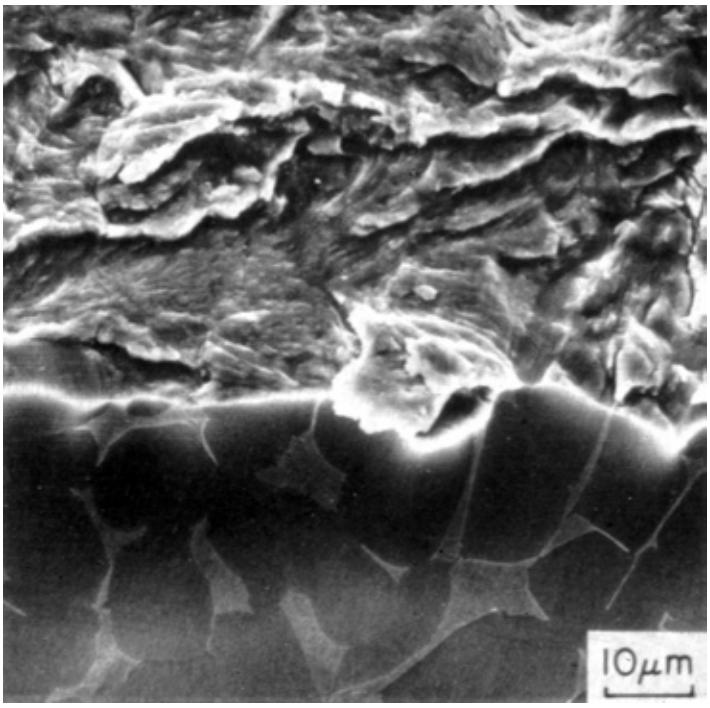

(Left) Technique of "plateau etch" of fracture surface (top) to reveal underlying microstructure of primary alpha grains in the "recrystallization anneal" or RA structure of Ti-6 Al-4 V.

Four photos courtesy J.C. Chesnutt

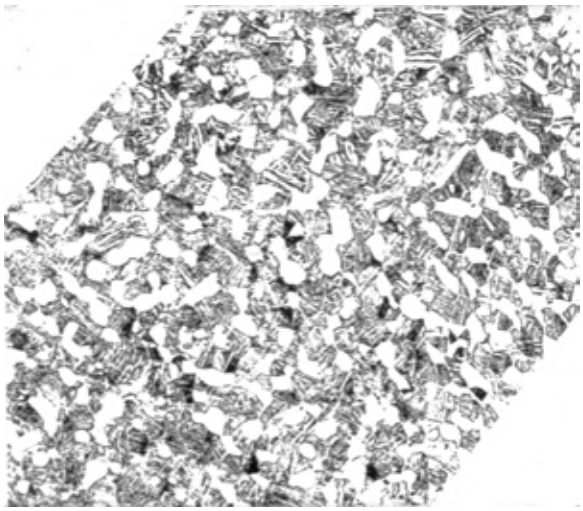

(Right) Three-dimensional representation of uniformity of microstructure in upset-forged Ti-6 Al-4 V, in the "solution treated and overaged" or STOA structure, with primary alpha grains in a matrix of alpha + beta phase.

(Below) Plateau etching to show correlation of fracture and microstructure features.

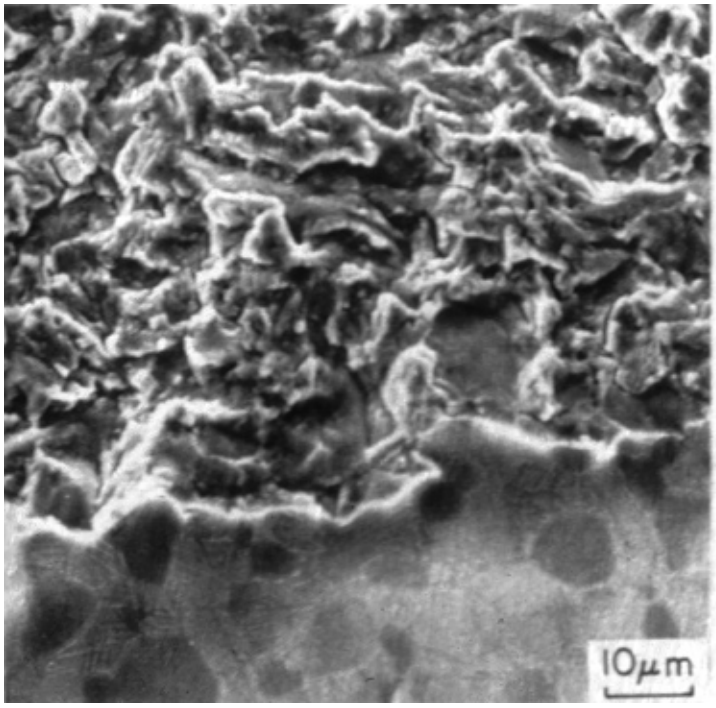

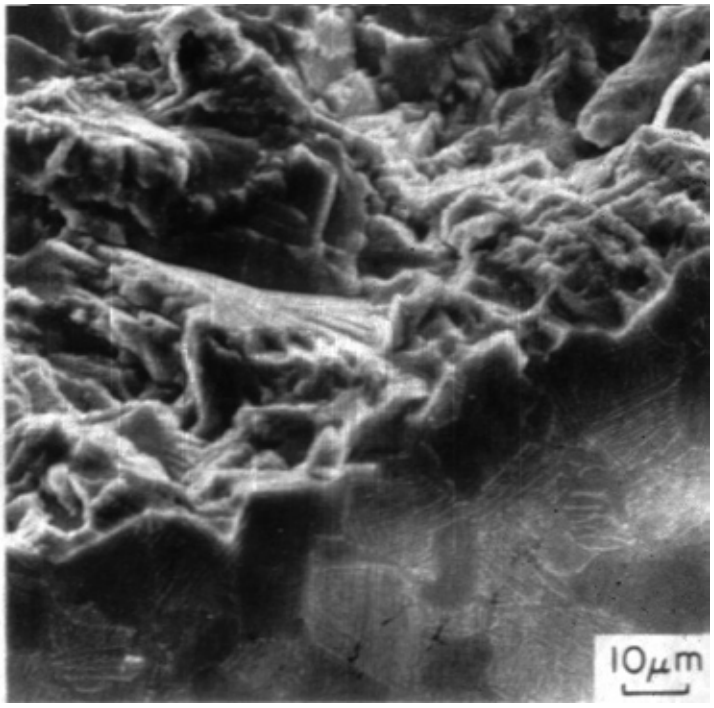

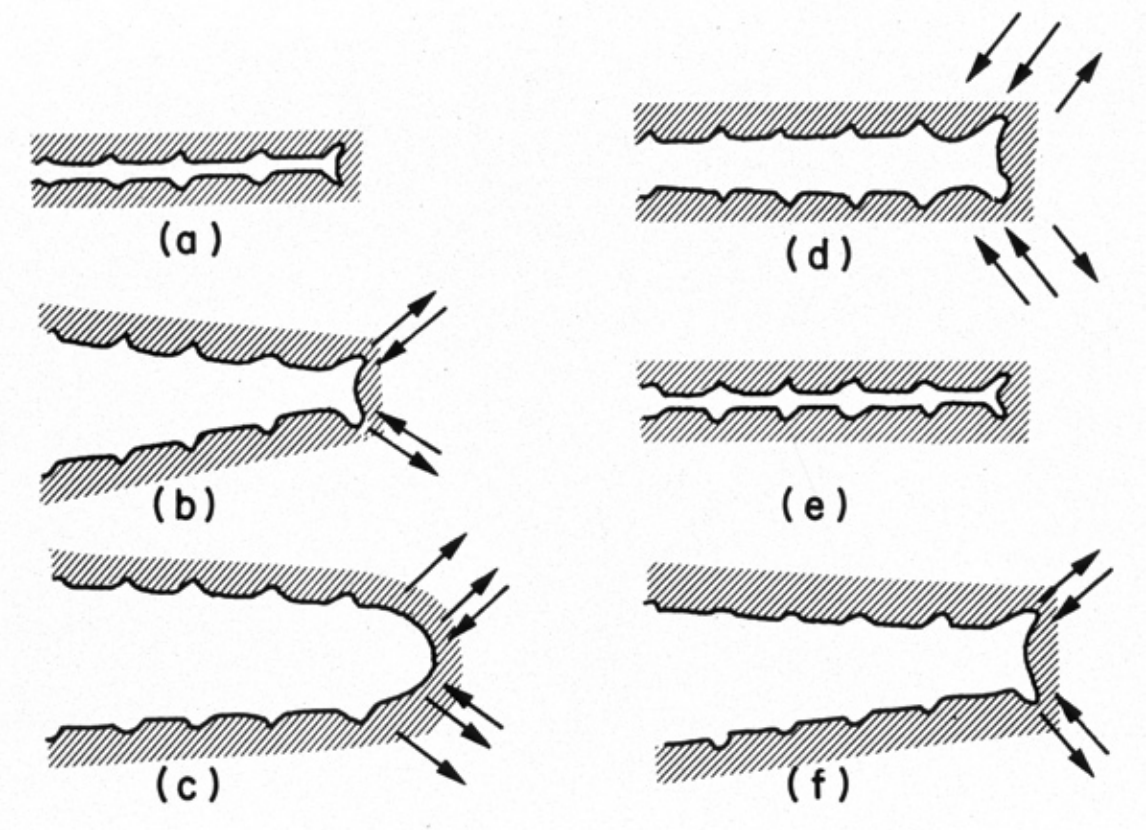

(Top) The sequence proposed by Laird for fully plastic generation of one striation per load cycle. From C. Laird, ASTM STP 415.

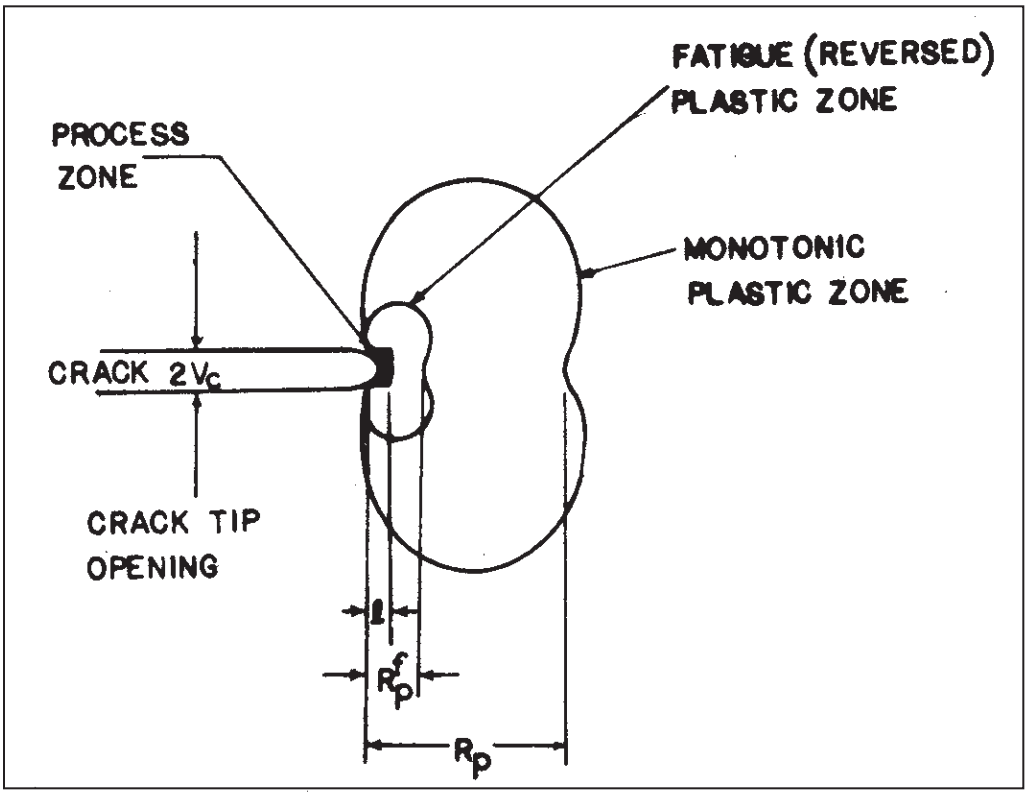

(Bottom) The "forward" or monotonic plastic zone, formed by the maximum stress in a fatigue loading cycle, has the familiar dimensions known from LEFM. Within it, however, is a fatigue zone, in which stress is fully reversed, and which is exactly one-fourth the size of the monotonic zone. Also shown is the process zone at the crack tip, where fracture processes are underway.

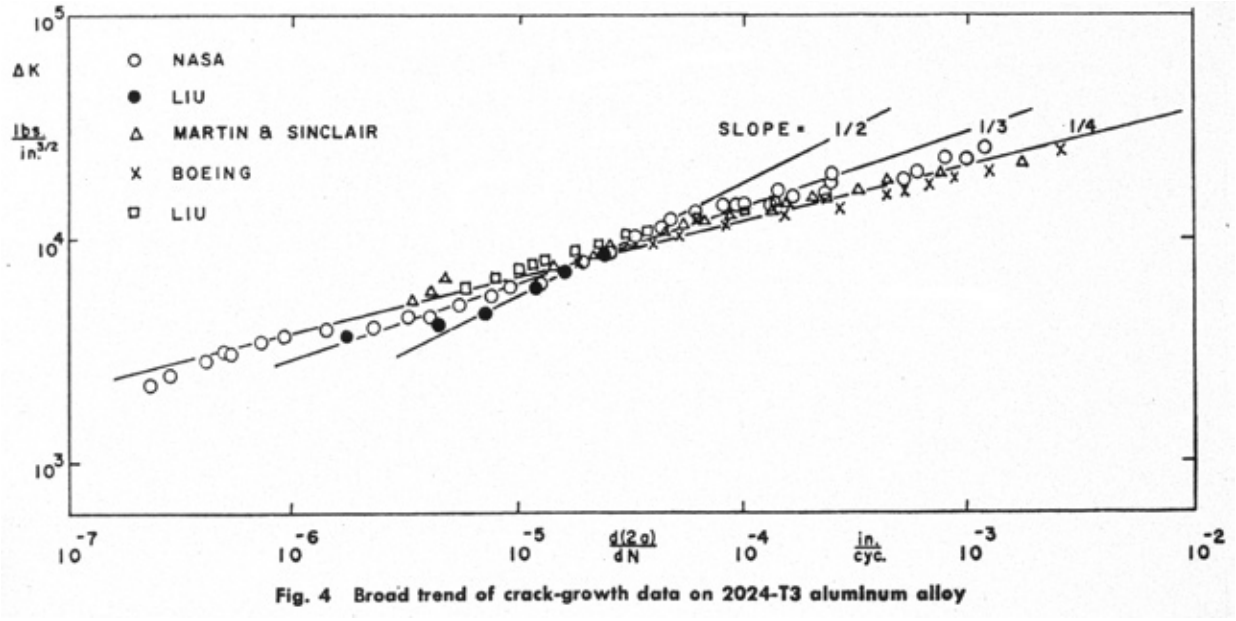

Fig. 4 Broad trend of crack-growth data on 2024-T3 aluminum alloy

(Above) The original Paris & Erdogan data on 2024 aluminum which led to the proposal of the "Paris Law," with *m* value about 4.

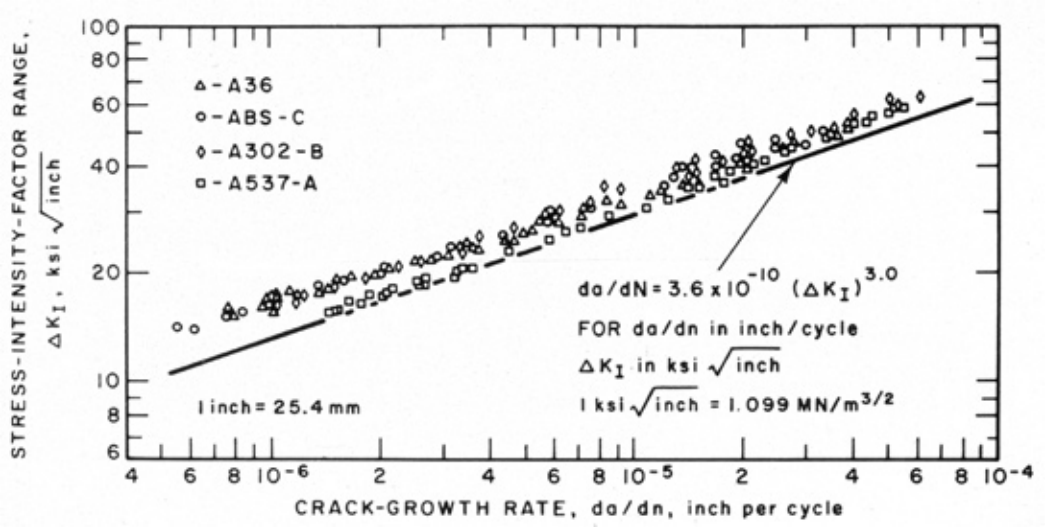

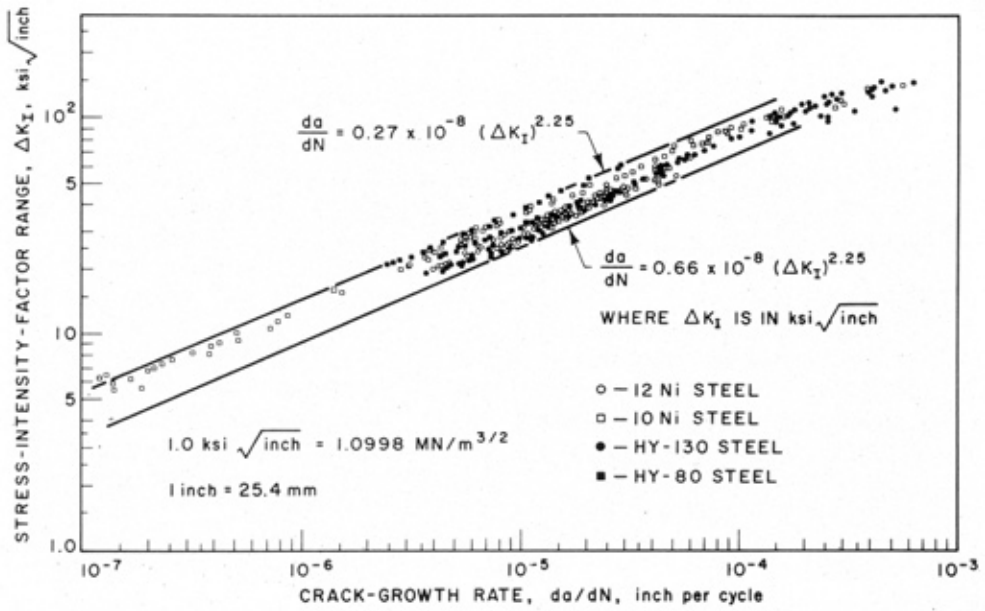

(Right) Collections of data by Rolfe and Barsom on steels of ferrite + pearlite microstructure, upper graph, and quenched and tempered martensitic steels of higher strength, lower graph. Note in all three figures on this page that the later convention of crack growth rate as the ordinate of such plots had not yet been accepted.

From S.T. Rolfe and J.M. Barsom, *Fracture and Fatigue Control in Structures*, Prentice-Hall, 1977, pages 237, 239.

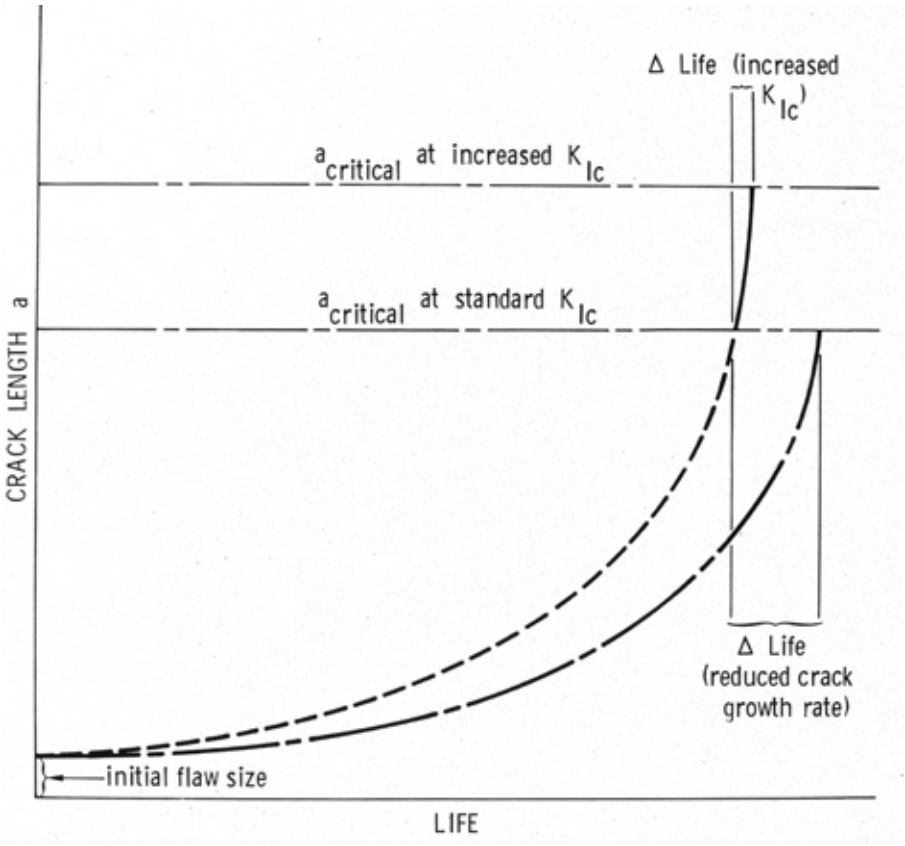

(Top) Illustration of how increases in fracture toughness, to extend the range of Stage III in the FCP diagram, produce far smaller gains in life, compared to reductions in FCP rate.

From Thompson.

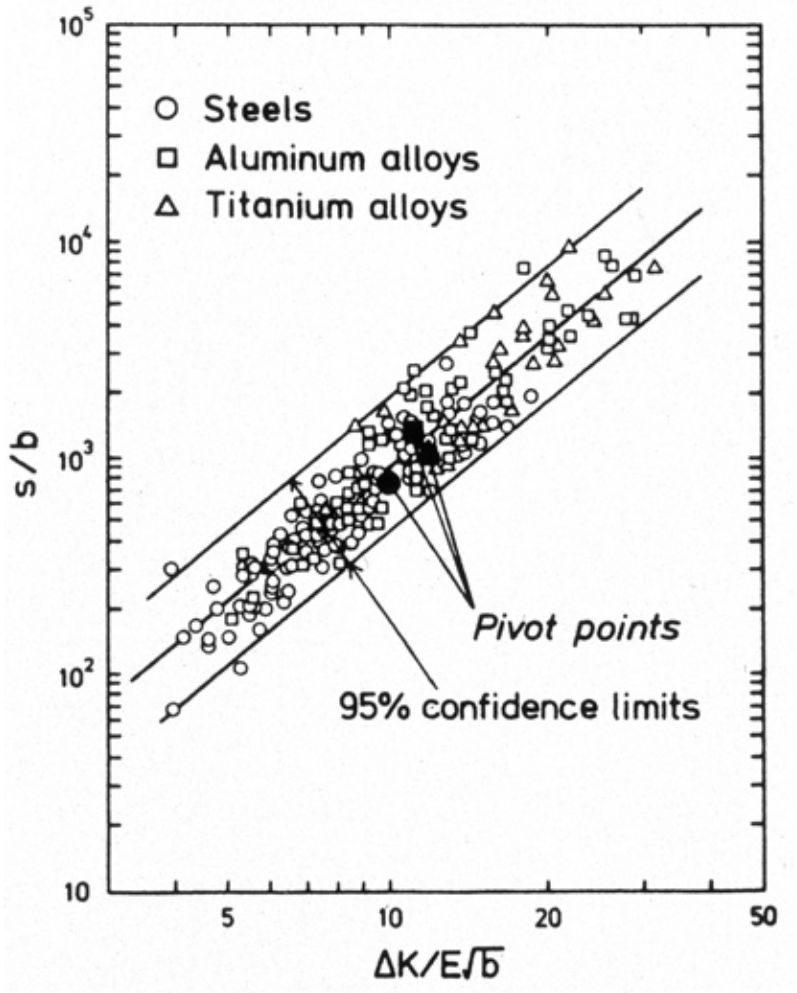

(Bottom) Collection of data on steels, titanium alloys, and aluminum alloys, showing how normalization with such factors as modulus E permits gathering data onto a single plot.

From Tanaka.

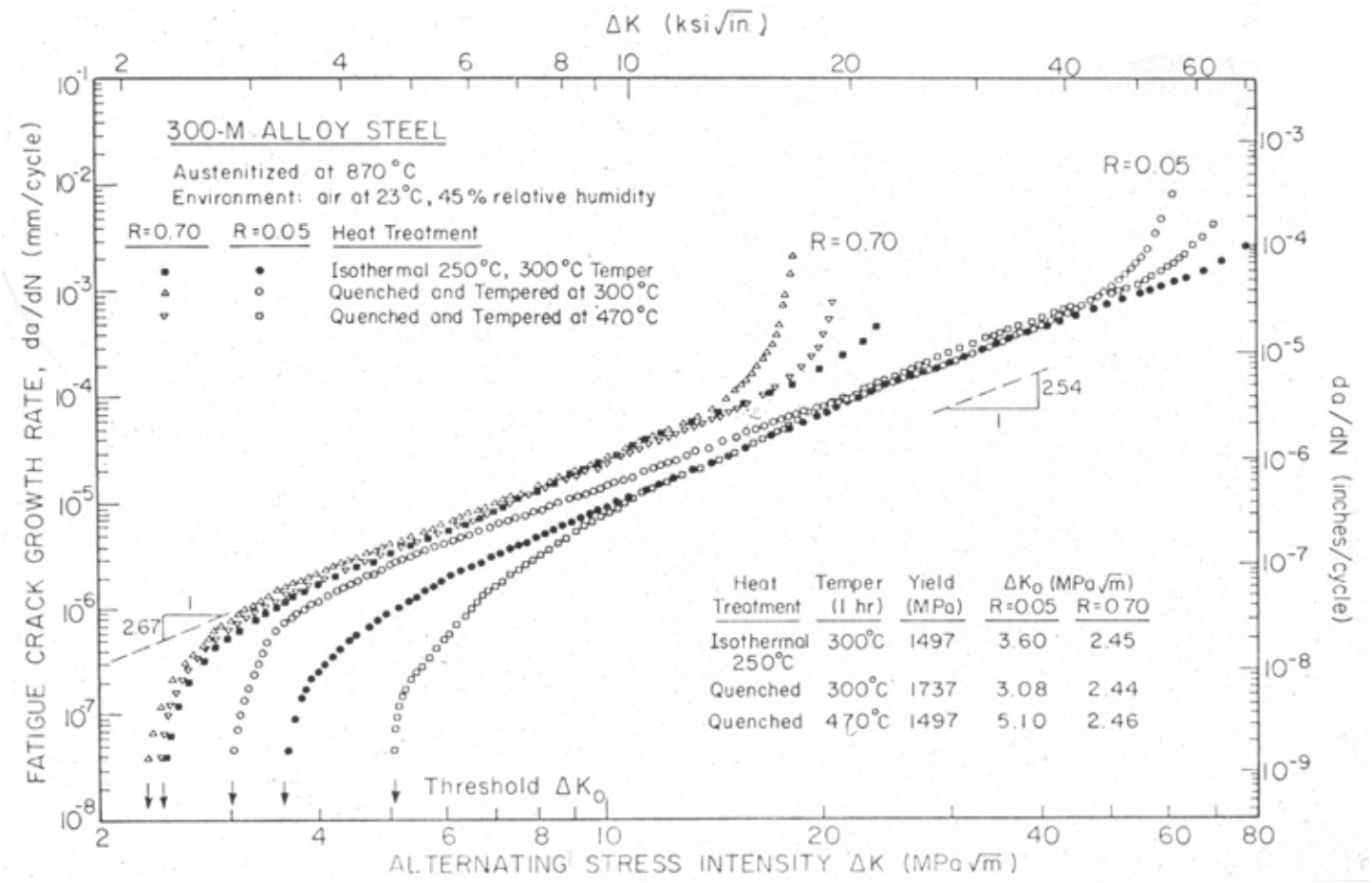

Data on steels, R.O. Ritchie, *Fracture 1977*

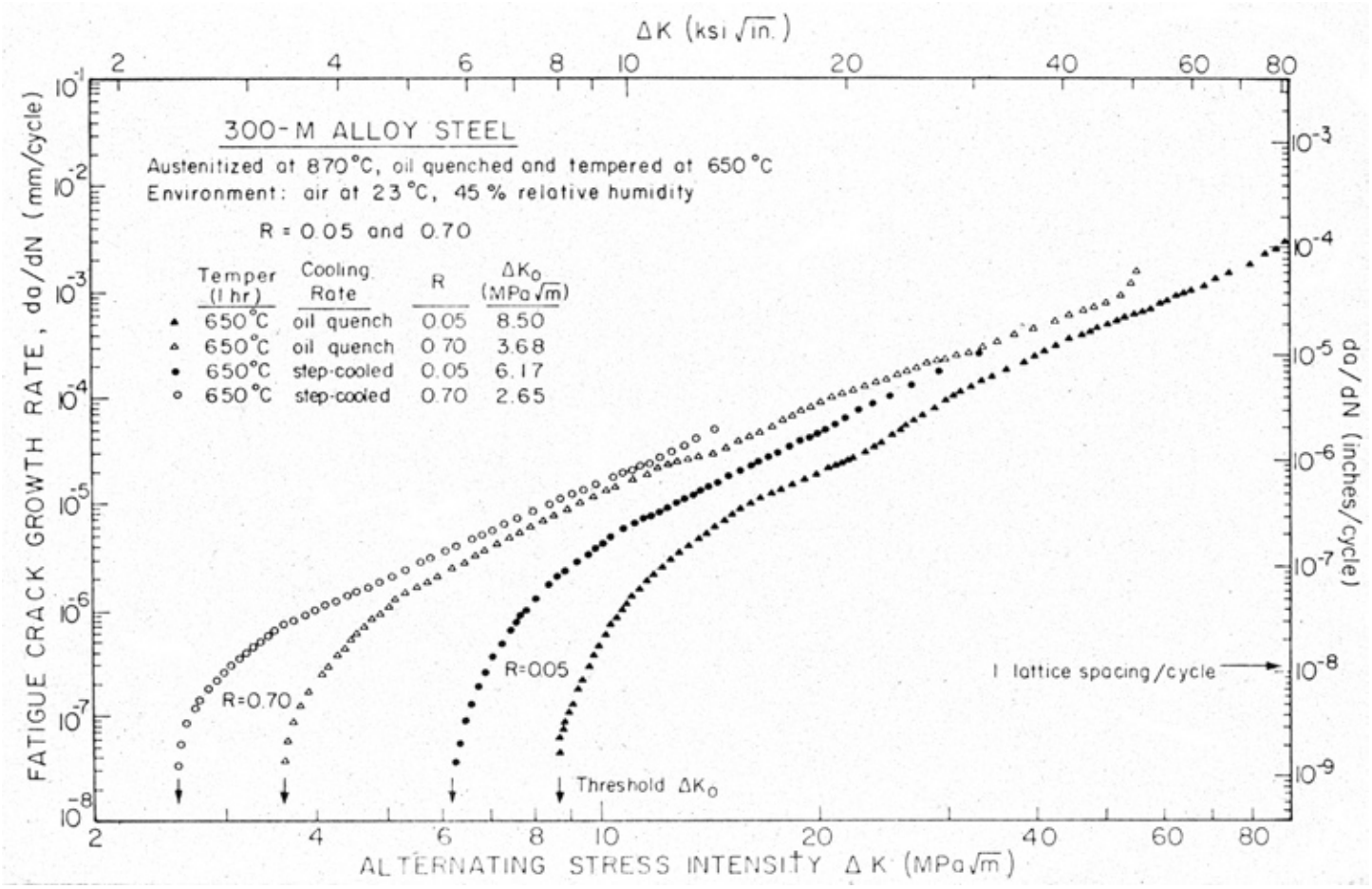

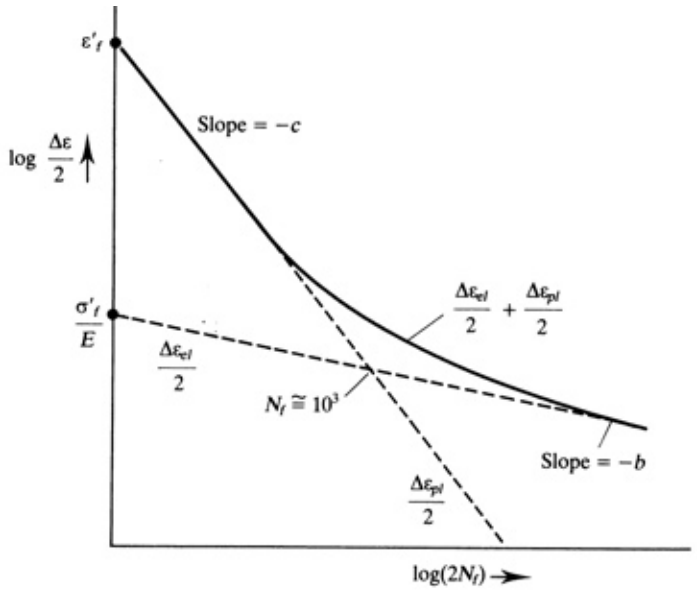

A schematic of the strain amplitude-number of stress (strain) reversals as given by Eq. (12.4). At low N_f values, $\Delta\varepsilon \cong \Delta\varepsilon_{pl}$ and the slope of the logarithmic coordinates employed is $-c$ and the intercept of the line is ε'_f. At high cycles the logarithmic slope is $-b$ (with $b < c$), and the extrapolation of this portion of the curve (where $\Delta\varepsilon \cong \Delta\varepsilon_{el}$) yields the intercept σ'_f/E.

(Top) Illustration of LCF at high strains per cycle, and HCF at essentially zero plastic strain per cycle, as end points on a diagram of strain range vs. life.

(From T. Courtney, *Mechanical Behavior of Materials*, p. 577

$$\tfrac{1}{2}\Delta\varepsilon = \tfrac{1}{2}\Delta\varepsilon_{el} + \tfrac{1}{2}\Delta\varepsilon_{pl} = \frac{\sigma'_f}{E}(2N_f)^{-b} + \varepsilon'_f(2N_f)^{-c}$$

(Below) Ratio of opening K to maximum K in the fatigue cycle, as a function of ΔK. If crack closure dominates the observation of crack growth threshold, then as this ratio approaches one, crack growth should stop, as seen here. From Minakawa & McEvily.

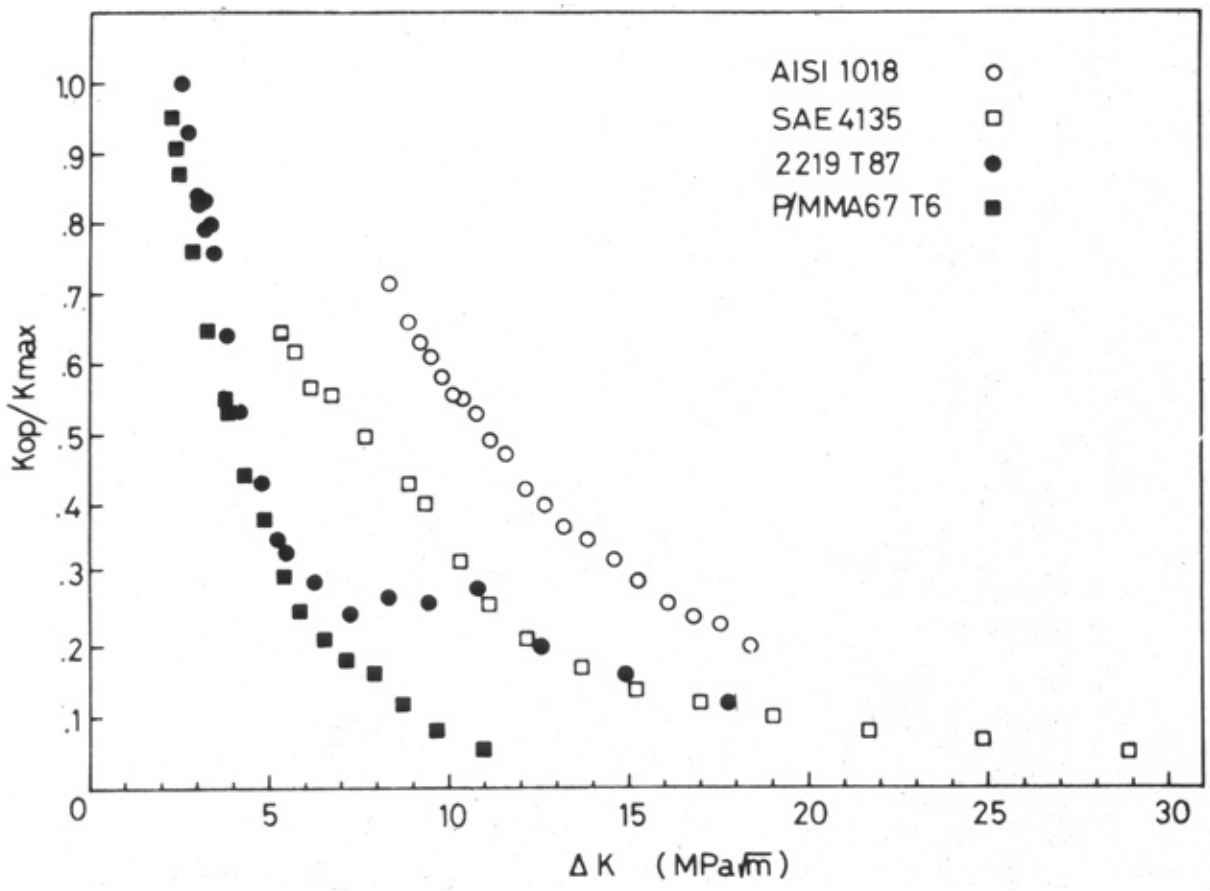

At right is shown a schematic representation of how crack nucleation and early growth at a stress concentrator may behave much like a low-cycle fatigue test, with a large plastic zone dut to the relatively large radius of the corner; but as the crack grows away from the concentrator, its plastic zone shrinks to the size associated with LEFM fatigue crack propagation.

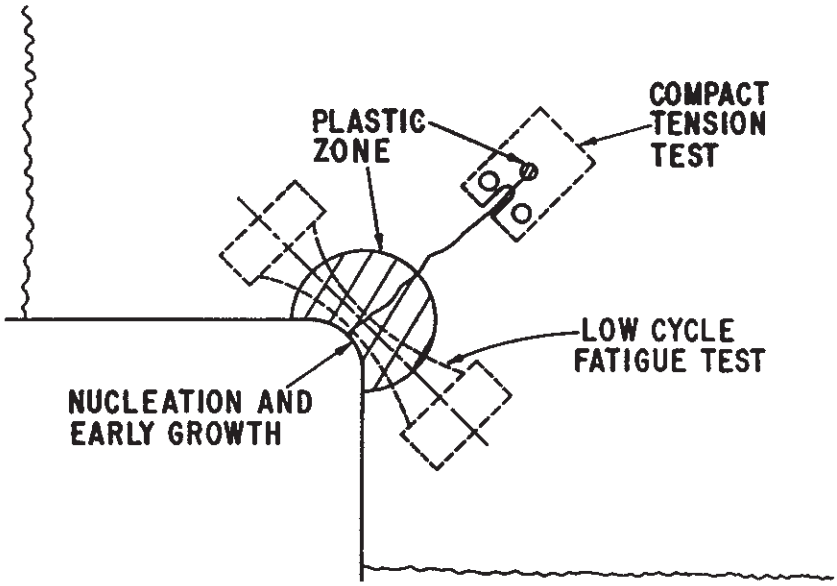

(Below) Often called a "Kitagawa" diagram for the researcher who gathered extensive data on the behavior, this graph shows in its right-hand part, the usual relation between crack length (to the one-half power) times stress, while the left-hand part shows simply the endurance limit: when cracks are too small for LEFM behavior, stress-controlled or long-life fatigue dominates, but if crack are large enough, stress intensity-controlled propagation to failure occurs.